

Surface Induced Smectic Order in Ionic Liquids — An X-Ray Reflectivity Study of $[\text{C}_{22}\text{C}_{1}\text{im}]^+[\text{NTf}_2]^-$

Julian Mars, Binyang Hou, Henning Weiss, Hailong Li, Oleg Konovalov, Sven Festersen, Bridget M. Murphy, Uta Rütt, Markus Bier, and Markus Mezger

Electronic Supplementary Information (ESI)

DSC

Phase transition temperatures were determined by differential scanning calorimetry (Mettler Toledo DSC-822) using scan rates of 1 K min^{-1} , 2 K min^{-1} , 5 K min^{-1} and 10 K min^{-1} . Equilibrium phase transition temperatures were obtained by extrapolating to zero heating and cooling rates respectively.

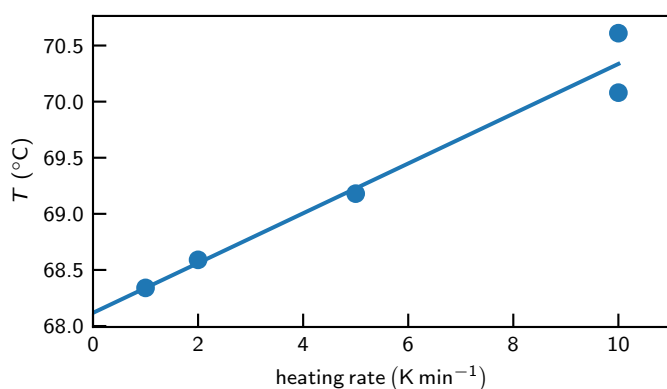


Fig. S1. (Color) Melting temperature determined by DSC heating rates of 1 K min^{-1} , 2 K min^{-1} , 5 K min^{-1} and 10 K min^{-1} . Equilibrium phase transition temperatures were obtained by extrapolating to zero heating rate.

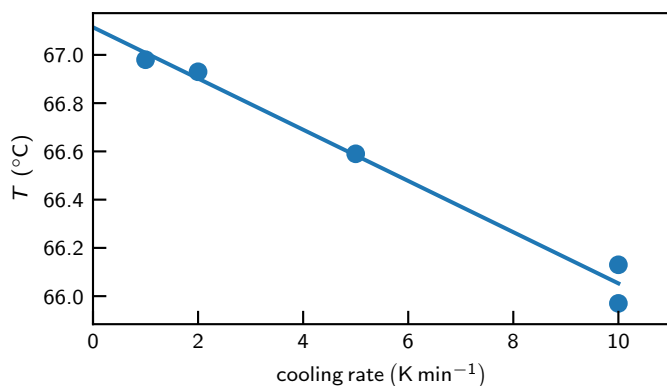


Fig. S2. (Color) Liquid crystalline transition temperatures T_{LC} determined by DSC cooling rates of 1 K min^{-1} , 2 K min^{-1} , 5 K min^{-1} and 10 K min^{-1} . Equilibrium phase transition temperatures were obtained by extrapolating to zero cooling rate.

XRR

Parameter space mapping revealed that the fits of the model to the XRR data are highly sensitive to smectic layer thickness L (Eq. 4). Fits have been performed for offsets of $\Delta L = -5 \text{ nm}$, -2 nm , -1 nm , 2 nm and 5 nm with respect to the best fit layer thickness L_0 . The decrease of the fit quality is quantified by the increase $\Delta = \chi_L/\chi_0 - 1$ of the cost function χ_L with respect to the best fit cost value χ_0 . Figure S3 clearly shows that with increasing temperature the minima of Δ , i.e., the best fit values for L , are shifting to smaller wetting layer thicknesses. Even for the highest temperature of 115°C investigated in this study, introducing a smectic layer significantly improves the fit.

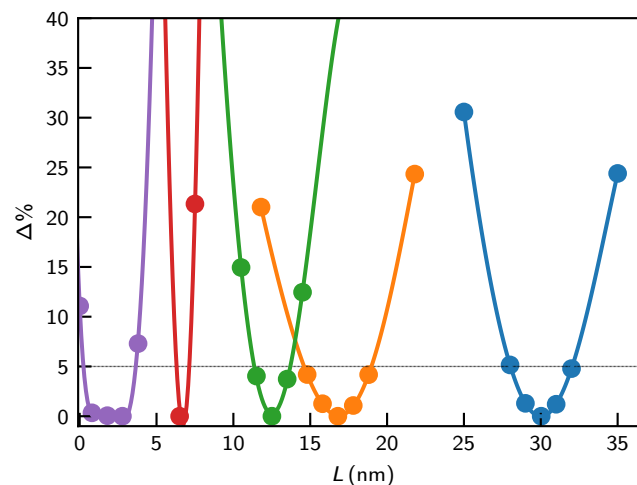


Fig. S3. (Color) Dependence of the fit quality on the smectic layer wetting thickness L for different temperatures (blue 68°C , orange 70°C , green 73°C , red 87°C and purple 115°C). Errors of the fit value L are estimated within a 5% range of the fit quality Δ (horizontal line).

In Fig S4a and Fig S4b exemplary reflectivity curves obtained for $\Delta L = -5 \text{ nm}$, -2 nm , 2 nm and 5 nm are shown. Particularly, the height to width ratio of the first quasi-Bragg is significantly influenced by ΔL .

For all values of $\xi_s \gg L$ fits of comparable quality were obtained. Here, the series expansion $\sinh(x) = x + \mathcal{O}(x^3)$ leads to a strong parameter coupling between ξ_s and S^- . Therefore, this parameter was fixed to $\xi_s = 2000 \text{ nm}$.

Analysis of the dependence on the surface tension γ are shown in Tab S1. The best fit parameters are only slightly affected by the assumptions for the surface tension (Tab. S1). In particular, a negligible influence on the smectic layer thickness L is found.

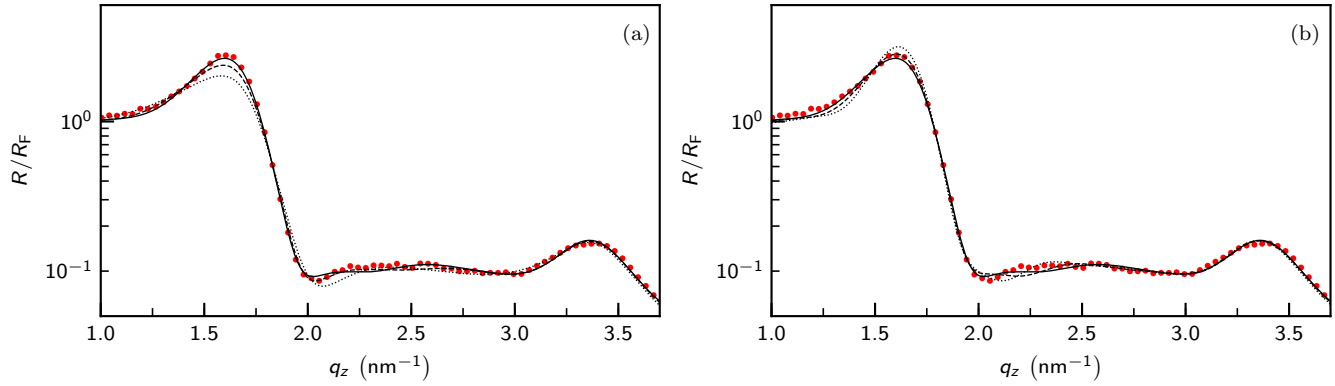


Fig. S4. (Color) Dependence of the fit on the smectic layer wetting thickness L for $73\text{ }^\circ\text{C}$. The solid line represents the best fit for $L = 12.5\text{ nm}$ ((a) and (b)). Profiles obtained for $\Delta L = -2\text{ nm}$ and -5 nm (a) and $\Delta L = 2\text{ nm}$ and 5 nm (b) are represent with dashed and dotted lines respectively .

Table S1. Comparison of fit parameters for different surface tensions γ at $73\text{ }^\circ\text{C}$

γ mN m^{-1}	L nm	ξ_b^\dagger nm	d nm	z_0 nm	σ_s nm	S^{0*}	S^-	B^*	a_2	ξ_2 nm
25	13.1	4.64	3.72	2.23	0.00	1.59	-179	7.02	0.18	12.5
30	12.5	4.64	3.73	2.24	0.10	1.62	-189	6.50	0.12	18.9
40	12.4	4.64	3.74	2.23	0.22	1.53	-179	6.06	0.10	18.6
60	12.4	4.64	3.74	2.23	0.30	1.44	-169	5.64	0.09	18.2

[†] Parameters were fixed to the interpolated bulk values extracted from SAXS. * Parameters were determined by continuity and differential continuity conditions. ξ_s was fixed at 2000 nm .